

METRIC PROPERTIES OF ROLLING SHUTTER LOW-ALTITUDE PHOTOGRAPHY

WŁACIWOSCI POMIAROWE ZDJĘĆ NISKOPUŁAPOWYCH POZYSKIWANYCH KAMERAŃ TYPU ROLLING SHUTTER

Zdzisław Kurczyński, Mateusz Bielecki

Department of Photogrammetry, Remote Sensing and Spatial Information Systems,
Faculty of Geodesy and Cartography, Warsaw University of Technology

KEY WORDS: rolling shutter, global shutter, aerotriangulation, UAS, UAV, low-altitude photogrammetry

SUMMARY: Remotely-controlled aircraft, together with acquisition of photographs from such platforms as well as generation and processing of acquired products, are all becoming more popular. These techniques are also more frequently and widely applied. Thus, "low-altitude photogrammetry" is becoming a rapidly-developing field. This popularity results from the wide accessibility of such platforms and from the availability of light and inexpensive photographic cameras and the computer software required for processing the photographs and generating useful products, among other things. The majority of photographic cameras use the CMOS type of sensors with electronic shutters of the rolling shutter type. Photographs from these cameras are geometrically distorted by shutter effect. The distortions may be modelled and corrected when the photographs are processed. This paper looks at distortions associated with rolling shutters. In the experimental part, 11 blocks of photographs from two test sites were adjusted; the photographs were acquired from the following UAS platforms: Quadcopter DJI Phantom 3 Professional and Quadcopter DJI Inspire One. Both platforms are equipped with Sony EXMOR cameras with electronic shutters. Blocks of photographs are characterized by different altitudes for data acquisition, overlap of photographs and the number of ground control. Using the Pix4Dmapper software tools the multi-variant block adjustment was performed, both with linear modelling of the rolling shutter effect and without such modelling. The obtained results are analysed. The validity and effectiveness of the linear modelling of the rolling shutter effect is discussed. The very high metric potential of low-altitude photographs is also presented.

1. INTRODUCTION

The methodology of metric processing of photographs is based on the assumption that, from the geometric perspective, such photographs are a central projection of a spatial object, (e.g., the terrain surface together with other objects) on the camera focal plane.

In the course of the development of photogrammetry, many efforts have been made to verify these assumptions in practice. Some of these efforts can be summarized as follows:

- The use of orthoscopic lenses which create images according to the central projection and the consideration of possible deviations from this assumption (radial and tangential distortion determined during the camera calibration process).
- The use of simultaneous action shutters (the entire frame is captured in each phase of opening and closing the shutter). Examples include central shutters, also known as "global shutters" (GS). Sequential shutters which progressively capture the frame are excluded. Focal-plane shutters are examples of such shutters that are commonly used by amateur photographers. This is important when the object is in motion relative to a fixed camera, or vice versa, as is the case when photographing the surface of the earth from a flying airplane.

At present, in the era of the common use of digital methods in photogrammetry, the above assumptions are differently formulated. Even high distortions of photographs in relation to mathematical central projections are permitted if they are determined in camera calibration processes and considered when photographs are processed; they may also be permitted by the processing methodology itself. Aerotriangulation with so-called additional parameters may be a good example; the residual errors in photographs are modelled, determined and considered during further processing (American Society of Photogrammetry and Remote Sensing, 2004, p.870, Kurczyński, 2014, p.503, Ziobro, 2012). This allows for the processing of non-metric photographs (acquired by non-photogrammetric cameras) even when the initial camera calibration is not performed.

These changes result in considerably wider groups of people dealing with generating products from photographs acquired by non-metric cameras. This is clearly seen in the rapid growth of photographs acquired from unmanned aerial vehicles (UAVs). Methods of processing such photographs are also rapidly growing. Software packages for processing photographs and for the generation of products such as orthophotomaps, digital terrain models or spatial (3D) models are becoming widely available. What we are actually seeing is the generation and development of "low-altitude photogrammetry" (Kurczyński et al., 2016).

UAV platforms are usually equipped with light and inexpensive photographic cameras and the software used for data processing is often designed for users who do not have much photogrammetric knowledge. Despite this, they are able to create valuable and useful products using highly automated processing which does not require highly-experienced operators.

This paper concerns the assessment of the metric potential of photographs acquired from UAV platforms and distorted by deformation caused by the RS (rolling shutter) types of cameras. The RS type shutter is a progressive action shutter, which means deformation of photos taken from a moving UAV platform.

2. ROLLING SHUTTER

The shutter is an important element of the camera which influences the image geometry. This influence must be considered when photographs are used for measurement or mapping purposes. From this perspective, the shutters of (analogue and digital) cameras may be divided into two categories, i.e., simultaneous action shutters and progressive action shutters.

In the case of cameras with simultaneous action shutters, the entire frame is exposed by the shutter at the same moment and the recorded frame is geometrically compliant with the geometry generated by the lens, i.e., with the central projection. The shutter does not introduce any additional image distortions. Such shutters are called global shutters (GS). They are used, among other types of shutters, in mapping cameras.

The so-called central shutter is a type of GS. It is used in analogue (film) cameras. The central shutter is built in to the lens and hence it is called a between-the-lens shutter. Such shutters are commonly used in aerial metric cameras. (American Society of Photogrammetry and Remote Sensing, 2004, p.584, Kurczyński, 2014, p. 58).

In digital cameras, GS shutters are often applied in connection with the image CCD (charge-coupled device) sensor. In such a sensor, each elementary pixel is accompanied by a memory cell. After exposing the CCD array, the electric charges stored in it are immediately transferred to the memory and then, after exposure, they are successively read out, enhanced, converted to the digital form (A/D conversion) and recorded. This means that an image created by the lens is not distorted in the recording process. Due to differences in the construction of CCD and CMOS (complementary metal–oxide–semiconductor) sensors these types of shutters are seldom used with CMOS (QImaging: [www](http://www.qimaging.com)).

In cameras with progressively-operating shutters the image is not created at the same moment over the entire frame; it is created progressively, line by line. If the object or the camera is moving at the time, the resulting image is highly geometrically distorted. Such shutters are called rolling shutters (RS).

In analogue cameras, such shutters are commonly used in single-lens reflex (SLR) cameras. The shutter is a slot which moves just in front of the film plane and progressively exposes the frame. For this reason, it is called a slot shutter or a focal-plane shutter. A very similar mechanical solution is used in DSLR (digital single-lens reflex) cameras.

The RS type of shutter may also be based on a purely electronic solution (an electronic shutter). This is often used in cameras equipped with CMOS arrays. At present, such cameras are becoming more popular. The camera is not equipped with a mechanical shutter which doses the light energy illuminating the sensor. The sensor is reset line by line, with a constant speed. After exposure, electric charges are readout line by line. This means that one line may be reset and another sensor line may be readout at the same time. The reading out of the entire array is distributed in time, specified as the rolling shutter readout time τ . (Ait-Aider et al., 2006, Mendonça, 2014, QImaging).

3. GEOMETRIC DISTORTIONS CAUSED BY THE ROLLING SHUTTER EFFECT

The spatial reconstruction of the bundle of rays which creates an image in the spatial coordinate system is the basis for metric processing of photographs from the spatial position of those rays at the moment the photograph was acquired. In the case of the central projection photograph this bundle of rays is determined by the so-called elements of the camera interior orientation (IO). Its position in space is determined by the exterior orientation (EO) elements. Six such parameters exist: three coordinates of the projection centre and three angles of the

photograph rotation. This is the case for cameras equipped with the GS type of shutter (Fig. 1a).

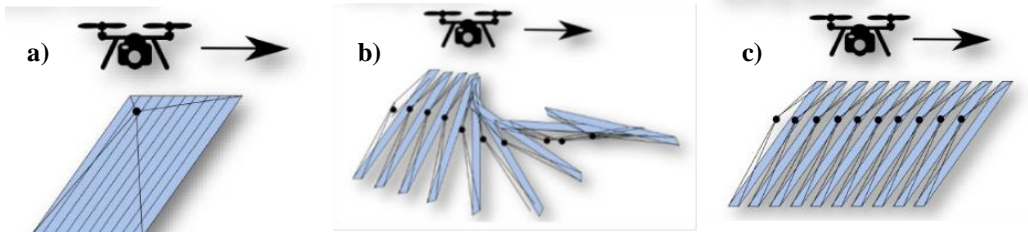


Fig. 1. The effect of the camera shutter on the image geometry: a) – the global shutter type of shutter with no image distortion, b) - the rolling shutter where both linear and angular elements of the photograph exterior orientation change at the time of exposure as a result of the platform movement and c) - the rolling shutter where only linear elements of the photograph orientation change at the time of exposure (Vautherin et al., 2016).

In the case of cameras with RS, the image is created line by line within a certain time τ . Since the camera is moving at the time of exposure, the exterior orientation elements are not constant. More accurately, the positions of the projection centre and the rotation angles are changing with time. This is illustrated in Fig. 1b. This causes obvious deviations of the photograph geometry from the central projection. Similar distortions occur in images acquired by means of push broom scanners.

The fundamental photogrammetric relation between the field coordinates of the point X and the coordinates of its image in the photograph x , acquired by a camera with the interior orientation elements π from the point c (the projection centre coordinates) and the rotation matrix R may be expressed in the following way (Vautherin et al., 2016):

$$x = \pi [R / - Rc] X \quad (1)$$

For a camera with an RS shutter (Fig. 1b) this expression will have the form:

$$x = \pi [R(t) / - R(t)c(t)] X \quad (2)$$

where:

- x - point coordinates in the photograph,
- X - point field coordinates,
- π - interior orientation elements,
- R - photograph rotation matrix,
- c - projection centre coordinates,
- t - timestamp of reading successive lines from the array of sensors.

In equation (2), which corresponds to the geometry of photographs with the RS effect, the values of the exterior orientation elements ($c(t)$ and $R(t)$) are expressed as functions of time.

The readout time of the sensor τ is relatively short; in popular cameras, it may be equal to 30 ms. Therefore, it is justified to assume that exterior orientation elements are changing linearly in that time. If so, the exterior orientation of a photograph is described by 12 parameters, instead of 6; six parameters for the first and six for the last line of the image.

Searching for further simplifications it may be seen that, as a result of the camera movement, only the position of the projection centre is changing and angular changes may be neglected. This will allow the fundamental equation to be simplified to the form:

$$x = \pi [R / - R c(t)] X \quad (3)$$

This simplification allows the exterior orientation elements of a photograph to be expressed using nine parameters. This is illustrated in Fig. 1c.

Image distortions caused by the RS effect may be expressed in pixels (Pix4D: www.pix4d.com/rolling-shutter-correction) as follows:

$$\Delta \approx \frac{V \cdot \tau \cdot f}{r \cdot H} \quad (4)$$

where:

- Δ - image shift (in pixels),
- V - velocity of the UAV platform,
- τ - readout time of the sensor for the entire frame,
- f - camera focal length,
- r - physical dimensions of a pixel,
- H - platform flight altitude above the ground.

For the Sony EXMOR 1/2.3" camera used in the experiment ($\tau=33$ ms, $f=3.55$ mm, $r=1.6 \mu\text{m}$) at a flight altitude $H=80$ m and a platform velocity $V=15$ m/s, the result is 18 pixels. For the fixed-wing platform with a typical velocity of 25 m/s the shift reaches 23 pixels.

These deformations should not be neglected in image processing for the purposes of measurement. One example of a software tool which accounts for this effect by means of linear modelling of the changes in exterior orientation elements is Pix4Dmapper.

4. PLANNING THE EXPERIMENTS

The objective of the experiments was to undertake practical tests of the influence of the RS effect. This was done by taking photographs over test fields, processing of blocks of photographs and analysis of RS effect reduction by means of linear modelling in the aerotriangulation process.

The experiment was performed for two test sites. Each of them was covered with strips of photographs acquired from different altitudes, with different end and side overlap and different RS effect modelling (with and without modelling). Multi-variant adjustment of the blocks of photographs was performed using Pix4Dmapper software.

Photographs were acquired from two UAV platforms (multicopters): Quadcopter DJI Phantom 3 Professional and Quadcopter DJI Inspire One, both equipped with RS cameras with similar parameters (CMOS sensor Sony EXMOR 1/2.3", resolution 12.4 Mpix, 4000x3000 pixels, pixel size 1.6 μm , $f=3.55$ mm, rolling shutter readout $\tau=33$ ms) (Fig. 2). All photos were taken in fix focus mode (lens manually focused on infinity).



Fig. 2. UAV platforms: Quadcopter DJI Phantom 3 Professional (left) and Quadcopter DJI Inspire One (right) (DJI: www.dji.com/phantom-3-pro/info#specs)

Test Site I

The first test site, with an area of about 1 km² and elevation differences up to 30 m has diversified land cover (village built-up areas, arable fields) (Fig. 3). This area was independently photographed nine times using a Quadcopter DJI Phantom 3 Professional at three flight altitudes: 80 m, 110 m and 150 m. Three independent flights with different coverages were performed from each altitude. Overlaps of 60/40%, 70/60% and 85/80% were applied. Table 1 presents the details of the planned flight parameters.

Table 1. Specifications of photographs acquired for Test Site I

| | | | | | | | | | |
|--------------------------|------|------|------|------|------|-----|------|------|------|
| Flight altitude [m]: | 80 | | | 110 | | | 150 | | |
| GSD [cm]: | 3,4 | | | 4,6 | | | 6,3 | | |
| Forward overlap [%]: | 60 | 70 | 85 | 60 | 70 | 85 | 60 | 70 | 85 |
| Side overlap [%]: | 40 | 60 | 80 | 40 | 60 | 80 | 40 | 60 | 80 |
| Number of strips: | 8 | 12 | 22 | 7 | 9 | 18 | 5 | 7 | 13 |
| Number of photos: | 164 | 350 | 1139 | 129 | 209 | 745 | 58 | 122 | 402 |
| Platform velocity [m/s]: | 14,0 | 10,8 | 7,3 | 13,0 | 13,0 | 9,7 | 15,2 | 12,9 | 12,7 |

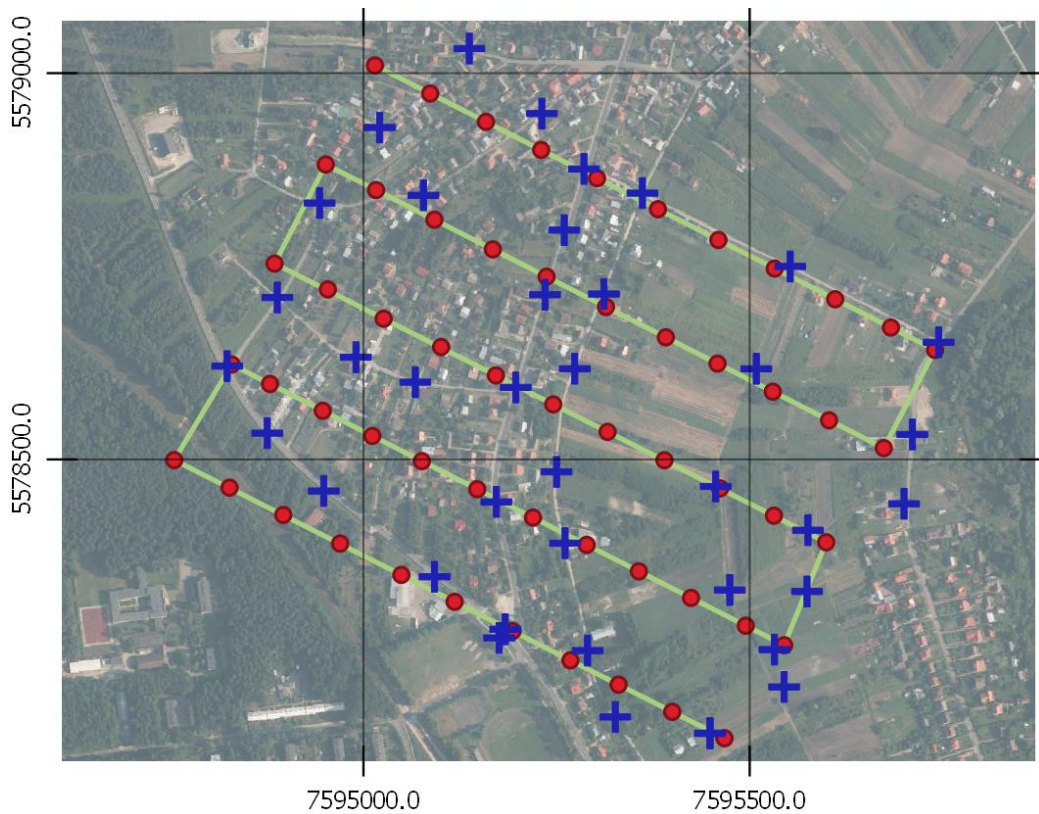


Figure 3. Test Site I. In the figure they are visible: positions of the photogrammetric ground control points (blue crosses) and strips with camera positions (red dots) for a flight altitude of 150 m and 60/40% of photo coverage

Altogether, 39 ground control points were designed, marked and measured within the area. The accuracy of determination of the coordinates is estimated as $RMS_{x,y} = 0.05$ m, $RMS_z = 0.10$ m (GNSS RTN method).

Test Site II

The second test site was a section of an expressway with a viaduct under construction. The area is elongated; its dimensions are 900 x 200 m. The height of the viaduct is approximately 10 m above the terrain surface. Independent flights at two altitudes 70 m and 90 m were performed using a Quadcopter DJIP Inspire One. In both flights, an overlap of 80/70% was applied. The object was covered with two blocks of photographs, with six strips in each block. The blocks contained 386 and 201 photographs, respectively.

For this test site, 28 ground control points were marked and measured within the area using electronic tacheometry; they were characterized by very high accuracy (RMS=0.003 m for all the coordinates).

The points were located on the terrain surface and on the viaduct under construction.

5. ADJUSTMENT OF THE BLOCKS OF PHOTOGRAPHS

Aerotriangulations of the acquired blocks of photographs for both test sites were performed in the Pix4Dmapper environment. Among other things, this environment supports:

- modelling of residual errors of photographs (aerotriangulation with additional parameters)
- two shutter models, i.e., GS (global shutter) or a shutter with linear modelling of the RS effect (linear rolling shutter).

For all blocks of photographs, the elements of the camera's interior orientation were treated as unknown. The basic elements were modelled (position of the principal point and camera focal length), and distortion parameters: three describing radial distortion and two describing tangential distortion. (American Society of Photogrammetry and Remote Sensing, 2004, p.872, Kurczyński, 2014, p.128). Previous camera calibration was not done. The adjustment was performed both without modelling the RS effect (the GS option) and with RS modelling (the linear rolling shutter option).

The bundle adjustment of each image block was executed a few times with different numbers of ground control points (GCPs). The remaining control points were considered as independent checkpoints (CPs). The comparisons of results and the accuracy analyses were performed based on independent checkpoint residuals. Synthetic results from the multi-variant aerotriangulation of photographs from Test Site I are presented in Table 2.

6. EVALUATION

The results from Test Site I show that:

1. The accuracy of horizontal position (RMS_{xy}) determined for checkpoints when there are four ground control points (GCPs) is worse than for the case of six or eight GCPs. The geodetic control consisting of eight GCPs may be considered sufficient. This is true for cases both with and without modelling of the RS effect. Further increase of the number of control points does not significantly improve accuracy.

2. For eight GCPs, with modelling of the RS effect, accuracy of horizontal position was achieved at the level of 0.9÷2.1 pixels (for different flight altitudes and different overlap variants). Such results may be considered highly satisfactory. For the same data, the accuracy achieved without modelling the RS effect was in the range of 3.4÷12.3 pixels.

These differences highlight the need for, and the efficiency of, linear modelling of the RS effect. It is worth noting that the increase in accuracy gained by modelling the RS effect was achieved for a moderate flight velocity of the UAV platform. For higher velocities, if the RS effect is not modelled, the errors would be greater.

Table 2. Test Site I. The accuracy of aerotriangulation at checkpoints for different photograph parameters (flight altitude, GSD, overlap of photographs), for different numbers of ground control points (GCPs) and for variants of the modelling methods for the RS effect. All errors are expressed in multiples of GSD

| Flight altitude GSD | Overlap | RMS | Errors on ground checkpoints [GSD] | | | | | |
|------------------------|---------|-------------------|------------------------------------|----------|----------|---------------|--------------------------|---------------|
| | | | Model: Rolling Shutter | | | | Model: Global Shutter | |
| | | | 4 GCP | 6 GCP | 8 GCP | 9 / 11 GCP | 4 GCP | 8 / 10 GCP |
| 80 m GSD=3.4 cm | 60/40% | RMS _{xy} | 4.2 | 3.0 | 2.1 | 1.9 | 9.3 | 7.5 |
| | | RMS _z | 8.5 | 3.5 | 5.3 | 7.0 | 15.4 | 4.3 |
| | 70/60% | RMS _{xy} | 3.6 | 3.0 | 1.6 | 1.5 | 11.8 | 12.3 |
| | | RMS _z | 27.7 | 15.0 | 6.4 | 6.2 | 134.9 | 10.5 |
| | 85/80% | RMS _{xy} | 7.9 | 2.8 | 2.1 | 1.9 | 9.9 | 8.5 |
| | | RMS _z | 45.3 | 23.7 | 12.0 | 8.0 | 18.8 | 12.7 |
| 110 m GSD=4.6 cm | 60/40% | RMS _{xy} | 3.4 | 1.7 | 1.6 | 1.6 | 4.7 | 3.9 |
| | | RMS _z | 5.5 | 0.5 | 4.2 | 4.9 | 4.1 | 2.7 |
| | 70/60% | RMS _{xy} | 1.7 | 1.5 | 1.1 | 1.1 | 4.4 | 4.0 |
| | | RMS _z | 23.9 | 11.0 | 5.2 | 3.0 | 7.8 | 4.4 |
| | 85/80% | RMS _{xy} | 6.8 | 2.2 | 1.8 | 1.4 | 9.5 | 8.0 |
| | | RMS _z | 18.1 | 13.9 | 7.2 | 5.6 | 59.0 | 6.9 |
| 150 m GSD=6.3 cm | 60/40% | RMS _{xy} | 3.1 | 2.1 | 1.7 | 1.6 | 3.6 | 3.4 |
| | | RMS _z | 8.4 | 4.8 | 2.4 | 1.4 | 6.1 | 2.4 |
| | 70/60% | RMS _{xy} | 2.7 | 1.8 | 0.9 | 3.7 | 3.7 | 3.4 |
| | | RMS _z | 10.1 | 26.5 | 3.7 | 15.0 | 15.0 | 6.8 |
| | 85/80% | RMS _{xy} | 1.5 | 1.4 | 0.9 | 0.9 | 1.9 | 4.7 |
| | | RMS _z | 5.4 | 0.7 | 2.9 | 3.4 | 5.4 | 3.1 |

3. The accuracy of elevation is different for different cases and, generally, it is worse than horizontal accuracy. Errors in the z coordinate (for eight GCPs) vary between 2.4 and 12.0 pixels with RS modelling and between 2.4 and 12.7 pixels without modelling. For poorer control (4÷6 GCPs) the errors are noticeably larger for both cases: with and without RS modelling. The results highlight significant elevation distortions in blocks of photographs. Only the geodetic control of eight GCPs stabilizes the elevation of the blocks of photographs. For this control, the mean error of elevation did not exceed 12 pixels for all cases. It is difficult to connect these errors with the flight parameters. There is no clear relation between the increased overlap and the increased elevation accuracy of the blocks of photographs. The worst results were obtained for the low flight altitude (80 m) and high coverage of photographs (85/80%). In conclusion, it is worth noting that these parameters were associated with a very large block (1139 photographs).
4. The lower elevation stability of blocks of photographs may be interpreted as the influence of modelling of systematic errors on the photographs (five parameters of distortion). Modelling of the camera interior orientation elements in the process of aerotriangulation results in the numerical instability of the adjustment, resulting from strong correlations between unknowns, including correlation of the focal length f and the parameters of radial distortion with the elevation of projection centres of the photographs. This may result in bigger errors in determining the f value which causes error in the altitude scale and, as a consequence, affine model deformations. This effect was more noticeable for the second test site.
5. Better horizontal and vertical accuracy expressed in pixels (GSD) can be observed for a higher flight altitude and for a larger GSD value, though the absolute accuracy expressed in meters is worse. This may be explained by the fact that in the case of a higher flight altitude and larger GSD value, errors in the field measurements of the geodetic control have relatively lower influence in the overall balance of errors. This is the case for Test Site I, where the estimated accuracy of the measurement of ground control points is relatively small, the position error exceeds the pixel size (GSD), especially for the lower flight altitudes.

Comparable results for Test Site II are presented in the Table 3. The results from Test Site II show that:

1. The accuracy of horizontal coordinates determined for checkpoints with four GCPs is similar for both flight altitudes and is equal to $RMS_{X,Y}=1.0\div 3.3$ pixels. For seven GCPs, subpixel accuracy is achieved.
2. The elevation accuracy is worse; the error is equal to several pixels for both variants of the geodetic control ($RMS_Z=2.6\div 8.3$ pixels). For some reason, better results were obtained for the block of photographs acquired from the higher altitude.
3. If the RS effect is not considered (the GS model) the elevation accuracy of the block of photographs deteriorates ($RMS_Z=11.5$ pixels), but there is no noticeable difference in the accuracy of horizontal coordinates.
The presence of systematic errors is visible (see value "mean"), especially in the variant without modeling of RS (Model GS).

Table 3. Test Site II. The accuracy of aerotriangulation at checkpoints for different photograph parameters (flight altitude, GSD, overlap of photographs), for different numbers of ground control points (GCPs) and for variants of the modelling methods for the RS effect. All errors are expressed in multiples of GSD

| Measure of accuracy | Coordinate | Errors on ground checkpoints [GSD] | | | | |
|---------------------|------------|-----------------------------------------------|-------|-----------------------------------------------|-------|-----------|
| | | GSD = 2.8 cm Alt. = 70 m Overlap 80/70% | | GSD = 4.0 cm Alt. = 90 m Overlap 80/70% | | |
| | | Model: Rolling Shutter | | | | Model: GS |
| | | 4 GCP | 7 GCP | 4 GCP | 7 GCP | 7 GCP |
| Mean | X | 0.9 | 0.1 | 0.6 | 0.1 | 0.8 |
| | Y | -1.2 | -0.3 | -2.5 | -0.4 | 0.6 |
| | Z | 3.5 | 4.0 | -2.7 | 1.0 | 6.0 |
| Sigma | X | 1.3 | 0.4 | 0.8 | 0.2 | 0.8 |
| | Y | 1.7 | 0.5 | 2.1 | 0.6 | 0.6 |
| | Z | 5.3 | 7.3 | 4.0 | 2.4 | 9.9 |
| RMS Error | X | 1.5 | 0.4 | 1.0 | 0.2 | 1.2 |
| | Y | 2.1 | 0.6 | 3.3 | 0.7 | 0.8 |
| | Z | 6.4 | 8.3 | 4.8 | 2.6 | 11.5 |

4. The above accuracy characteristics point to the metric possibilities of photographs acquired using an RS type camera from a UAS platform. For sufficient geodetic control (at the level of seven ground control points) an accuracy of horizontal coordinates of 1 pixel (or even subpixel accuracy) may be achieved. The elevation accuracy is several times worse. If the RS effect is not considered, elevation deformations of the block are increased.
5. A more detailed analysis of deviations for particular checkpoints confirms the surface distribution of deformations in the block, in particular, deformations of elevation. For a block acquired from a height of 70 m these deviations may have large values, and may reach 34 pixels (as the maximum) for the variant with four GCPs and 17 pixels for the variant with seven GCPs, all GCPs located on the ground (no GCP on the viaduct). For the block acquired from 90 m the deformations are smaller; up to 8 pixels (as the maximum for four GCPs) and 5 pixels (for seven GCPs).
6. High and systematic deformations of elevation were observed at checkpoints located on the viaduct (about 10 m above the terrain surface), in particular in the block of photographs acquired from the lower altitude. Deviations at checkpoints located on the viaduct were large, systematic and almost identical in the range of 12÷17 pixels for both variants of the geodetic control (four and seven GCPs).
This may suggest the block affine deformations resulting in an incorrect scale for the elevation. Such an effect may be caused by the strong correlation of the camera focal length (considered as the unknown in the adjustment process) and the altitude of the projection centres of the photographs, for the case of small height differences in the field.

These conditions occur in the discussed experiment when the aerotriangulation block is adjusted with additional parameters, (i.e., when interior orientation elements are considered as the unknowns) and with all GCPs located on the ground (no GCP on the viaduct). This may lead to numerical instability in the process of adjustment and unsatisfactory determination of the above-mentioned focal length and correlated unknowns. In order to confirm this assumption, the additional adjustment was performed (for both flight altitudes), with the replacing of two GCP on the ground surface by the another GCP located on the viaduct. This resulted in considerable improvement of the elevation accuracy of blocks of photographs for both flight altitudes (70 m and 90 m). Deviations in the block do not exceed 5 pixels for 70 m and 4 pixels for 90 m; they achieve subpixel values on checkpoints located on the viaduct. This confirms the well-known photogrammetric recommendation that the field control should encompass both horizontal and elevation range of the object.

7. CONCLUSIONS

The number of UAS users is rapidly growing and photographs acquired from such platforms are more frequently used for mapping purposes.

The popularity of such photographs is influenced by the accessibility of platforms equipped with inexpensive digital cameras and the growing availability of software tools for processing and generating basic products such as orthophotomaps, elevation models, vector maps or spatial (3D) models of objects. We are witnessing the birth of "low-altitude photogrammetry".

Some limitations of metric processing of such photographs result from their geometry, as influenced by the rolling shutter effect which deforms the photographs. This effect may be, to some extent, modelled and included in the processing.

Experiments were performed for many blocks of photographs with different parameters (the flight altitude, the forward and side overlap of photographs), acquired above two test sites. These experiments prove the effectiveness of modelling the RS effect and the metric possibilities of low-altitude photographs. Photographs were processed using Pix4Dmapper software which allows for linear modelling of the RS effect. Modeling of the RS effect allows to reduce the horizontal errors in the aerotriangulation block up to 6 times compared to the case without such modeling. Improving the elevation accuracy when modeling the RS effect is not as clear.

The correct planning and implementation of aerial photogrammetric work and the correct processing of the photographs allows to achieve processing accuracy at the level of single pixel (GSD), i.e., an accuracy similar to that which may be achieved with the use of professional, highly-expensive, large-format aerial cameras. However, the efficiency and productivity of these alternative source of image data is still under discussion. There is no doubt that low-altitude photogrammetry is a very attractive solution for small objects, and in particular for objects which require multi-temporal data acquisition.

LITERATURE

Ait-Aider O., Andreff N., Lavest J. M., Blaise U., Ferr P. C., and Cnrs. L. U., 2006. Simultaneous object pose and velocity computation using a single view from a rolling shutter camera. *Proc. European Conference on Computer Vision*, pp. 56–68.

American Society of Photogrammetry and Remote Sensing, 2004. *Manual of Photogrammetry*, Fifth Edition, 2004.

Kurczyński Z., 2014. *Fotogrametria*. PWN, 2014.

Kurczynski Z., Bakula K., Karabin M., Kowalczyk M., Markiewicz S., Ostrowski W., Podlasiak P., Zawieska D., 2016. The possibility of using images obtained from the UAS in the works concerning the land and buildings registration. *The International Archives of the Photogrammetry, Remote Sensing and Spatial Information Sciences* 41, 909-915.

Mendonça H., 2014. Rolling Shutter Bundle Adjustment. Master's Thesis. University of Zurich, 2014.

Vautherin J., Rutishauser S., Schneider-Zapp K., Fai Choi H., Chovancova V., Glass A., Strecha C., 2016. Photogrammetric Accuracy and Modeling of Rolling Shutter Cameras. *ISPRS Annals of Photogrammetry, Remote Sensing and Spatial Information Sciences*, 3, 139-146.

Ziobro J., 2012. Wykorzystanie pomiaru GNSS/IMU w krajowych aerotriangulacjach. *Archiwum Fotogrametrii, Kartografii i Teledetekcji* 23, 531–539.

Pix4D: www.pix4d.com/rolling-shutter-correction

DJI: www.dji.com/phantom-3-pro/info#specs

QImaging: www.qimaging.com

WŁACIWOSCI POMIAROWE ZDJĘĆ NISKOPULAPOWYCH POZYSKIWANYCH KAMERAŃ TYPU ROLLING SHUTTER

SŁOWA KLUCZOWE: Rolling Shutter, Global Shutter, aerotriangulacja, UAV, fotogrametria niskiego pułapu.

Streszczenie

Rośnie popularność zdalnie pilotowanych statków powietrznych oraz fotografowania z takich platform dla tworzenia produktów pochodnych z ich opracowania zdjęć. Znajdują one coraz powszechniejsze zastosowania. Rodzi się „fotogrametria z niskiego pułapu”. Ta popularność bierze się między innymi z łatwej dostępności do samych platform, lekkich i tanich kamer fotograficznych oraz programów komputerowych do opracowania zdjęć i wytwarzania z nich użytecznych produktów. Większość z używanych kamer fotograficznych oparte jest na przetwornikach obrazowych typu CMOS z migawkami elektronicznymi typu „Rolling Shutter”. Zdjęcia takie obarczone są zniekształceniami geometrycznymi. Zniekształcenia te można modelować i uwzględniać w procesie opracowania. W artykule przybliża się charakter zniekształceń typu *rolling shutter*. W części eksperymentalnej poddano wyrównaniu 11 bloków zdjęć nad dwoma obszarami testowymi, pozyskanych z platform UAS: Quadrokopter DJI Phantom 3 Professional i Quadrokopter DJI Inspire One, obie wyposażone w kamery Sony EXMOR z migawką elektroniczną. Bloki różniły się wysokością fotografowania, pokryciami zdjęć i połową osnową fotogrametryczną. Wykorzystując oprogramowanie Pix4DMapper dokonano wielowariantowego wyrównania bloków z liniowym modelowaniem efektu *rolling shutter* i bez takiego modelowania. Wyniki poddano analizie. Stwierdzono zasadność i skuteczność liniowego modelowania efektu *rolling shutter*. Wykazano bardzo duży potencjał pomiarowy zdjęć niskopułapowych.

Dane autorów / Authors' details:

dr hab. Zdzisław Kurczyński, prof. PW
kurczynski@wp.pl
telefon: 22 234 7694

inż. Mateusz Bielecki
geomat.bielecki@gmail.com

Przesłano / Submitted 29.10.2017
Zaakceptowano / Accepted 31.12.2017